



## Microstructure, mechanical properties and wear behaviour of Zn–Al–Cu–TiB<sub>2</sub> in situ composites

Fei CHEN, Tong-min WANG, Zong-ning CHEN, Feng MAO, Qiang HAN, Zhi-qiang CAO

School of Materials Science and Engineering, Dalian University of Technology, Dalian 116024, China

Received 21 February 2014; accepted 26 May 2014

**Abstract:** Zn–Al–Cu–TiB<sub>2</sub> (ZA27–TiB<sub>2</sub>) in situ composites were fabricated via reactions between molten aluminum and mixed halide salts (K<sub>2</sub>TiF<sub>6</sub> and KBF<sub>4</sub>) at temperature of 875 °C. The microstructure, mechanical properties and wear behavior of the composites were investigated. Microstructure analysis shows that fine and clean TiB<sub>2</sub> particles distribute uniformly through the matrix. The mechanical properties of the composites increase with the increase in TiB<sub>2</sub> content. As TiB<sub>2</sub> content increases to 5% (mass fraction), an improvement of HB 18 in hardness and 49 MPa in ultimate tensile strength (UTS) is achieved. The overall results reveal that the composites possess low friction coefficients and the wear rate is reduced from  $5.9 \times 10^{-3}$  to  $1.3 \times 10^{-3}$  mm<sup>3</sup>/m after incorporating 5% TiB<sub>2</sub>. Friction coefficient and worn surface analysis indicate that there is a change in the wear mechanism in the initial stage of wear test after introducing in situ TiB<sub>2</sub> particles into the matrix.

**Key words:** in situ composites; TiB<sub>2</sub> particles; friction coefficient; wear rate; mechanical properties

### 1 Introduction

The zinc-based alloys containing aluminum, copper and magnesium are characterized by high strength, excellent tribological properties and low melting temperatures, thus having potential for replacing the traditional bronze and iron base foundry alloys to produce wear resistant components [1,2]. In recent years, reinforcing with second phase particles has been noted to substantially improve the mechanical properties and wear response of zinc-based bearing materials. Conventional preparation of zinc-based composites involves the addition of externally synthesized particles, for instance, SiC [3], Al<sub>2</sub>O<sub>3</sub> [4], ZrO<sub>2</sub>, graphite [5] and TiO<sub>2</sub> [6] into molten matrix. Various problems, such as particles segregation and poor adhesion at the interface and inferior thermodynamically instability of the reinforcement frequently arise owing to surface contamination of the reinforcements and poor particle–matrix wettability.

Recently, in situ fabrication techniques have been developed to produce metal matrix composites (MMC). Since the formation and growth of reinforcement take

place within the matrix, in situ preparation of composites provides advantages including uniform distribution of finer particles, excellent bond at the interface, thermodynamically stable reinforcements that overwhelm the conventional ex situ processes, yielding better mechanical and tribological properties. Although various in situ techniques have been used to fabricate aluminum [7–9], magnesium [10], copper [11], iron [12] base MMC, fewer studies have been reported regarding the fabrication and properties of zinc-based in situ composites.

The present work focuses on the fabrication, microstructure, mechanical properties and wear behaviour of TiB<sub>2</sub> particulate reinforced ZA27 in situ composites synthesized by mixed salt route. TiB<sub>2</sub> is an advanced reinforcement for zinc-based composites as it possesses a useful combination of physical and mechanical properties, including high melting point (3225 °C), high elastic modulus (534 GPa), high hardness (HV 960) and outstanding wear resistance. More importantly, it does not react with zinc or aluminum to form reaction product at the interface between reinforcement and matrix [13,14]. ZA27 alloy, the nominal composition listed in Table 1, was selected

**Table 1** Chemical composition of ZA27 alloy (ASTM B 240–2004) (mass fraction, %)

Al	Cu	Mg	Zn
25.5–28.0	2.0–2.5	0.012–0.020	Bal.

as the matrix alloy because. On one hand, it has been considered for a number of commercial applications due to good mechanical properties, machinability and wear properties [15,16]; on the other hand, aluminum in ZA27 helps to facilitate the salt reaction via aluminothermy reduction in the synthesis process.

## 2 Experimental

ZA27–TiB<sub>2</sub> in situ composites were produced in the laboratory by mixed halide salt reaction. Commercial pure aluminum (99.7%) was melted and heated to 875 °C in a graphite-clay crucible with a resistance furnace. Pre-dried K<sub>2</sub>TiF<sub>6</sub> and KBF<sub>4</sub> salts, weighed at a stoichiometric ratio Ti to B of 1:2, were fully blended and wrapped with aluminum foil. A small amount of KCl, CaCl<sub>2</sub> and Na<sub>3</sub>AlF<sub>6</sub> salts were added as the reactive assistant and covering agent. The mixed salts were then pressed into the melt and stirred thoroughly for 30 s. The melt was held at 875 °C for 45 min to allow the reaction to reach completion. Cu and Mg were added in the form of Al–Cu and Al–Mg master alloys, whilst Zn was added in the form of molten zinc. After removing the slag and degassing by refining flux and high-purity argon, the melt was poured into a preheated thin-wall permanent mold. A total of three composites (see Fig. 1(a)) were produced with different mass fractions of TiB<sub>2</sub> (1%, 3% and 5%). The chemical composition of the composites was determined by atomic absorption analysis.

X-ray diffraction (XRD) test was carried out with a Shimadzu XRD–6000 to identify the various phases in the composites. The microstructures of the composites were examined with a Zeiss Supra 55 scanning electron microscope (SEM). Hardness tests of the composites were carried out by a Brinell hardness tester. The tensile specimens were prepared according to ASTM E8M–04 standard having a gauge length of 30 mm, a gauge diameter of 6 mm. The tensile strength was estimated with a computerized universal testing machine at room temperature and the strain rate for tensile test was  $1.25 \times 10^{-3} \text{ s}^{-1}$ . The present values of the hardness and tensile properties are the average of three tests for each composite. The fracture surfaces of the failed tensile specimens were analyzed by SEM.

Wear tests were carried out at room temperature with a computer-controlled pin-on-disc wear testing machine, and the schematic diagram of the wear test is shown in Fig. 1(b). The pins with 4.8 mm in diameter and 12.7 mm in length were machined from ZA27 alloy

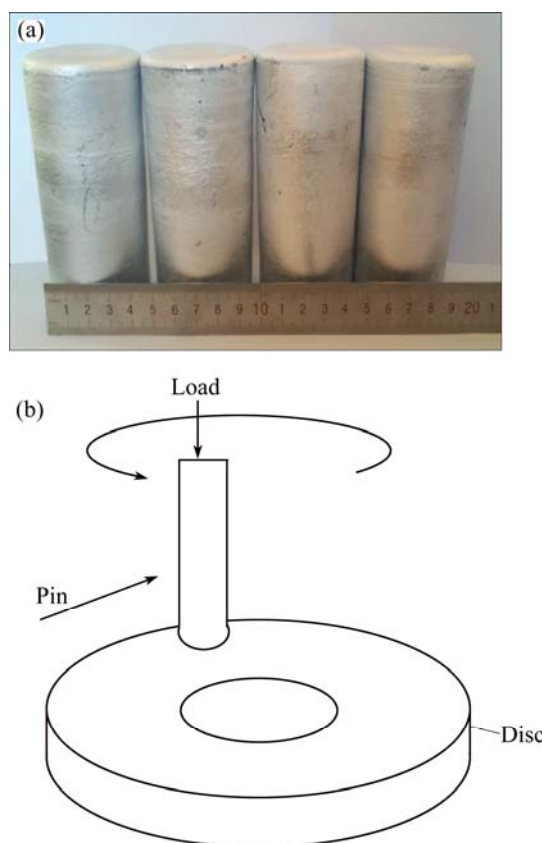


**Fig. 1** Ingots of matrix alloy and composites (a) and schematic diagram of pin-on-disc wear test (b)

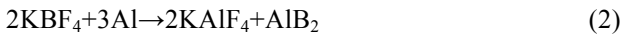
and the in situ MMC. The counterpart discs with an external diameter of 54 mm were made of SAE1045 steel (Fe–0.46%C–0.6%Mn–0.035%P–0.03%S) and had a hardness of HRC 50 after induction quenching. Wear tests were performed at a constant load of 90 N, which corresponded to a nominal contact stress of 5 MPa. For each sample, the wear test was carried out at a constant sliding speed of 0.75 m/s for 1 h (corresponding to a sliding distance of 2.7 km). SAE 40 oil was used as the lubricant. Each wear sample was ultrasonically cleaned in acetone and weighed before and after the test by an electronic balance with an accuracy of 0.1 mg to determine the mass loss. The wear rate was calculated by dividing the mass loss by sliding distance and measured density of the sample. The friction coefficients of the samples were recorded simultaneously by the computer. Three tests were carried out for each set of sample to get representative data. The worn surfaces were analyzed by SEM.

## 3 Results and discussion

### 3.1 Phase composition and microstructure of composites

The XRD patterns of the base alloy and the

developed in situ composites with different mass fractions of TiB<sub>2</sub> are shown in Fig. 2. The main phases of the composite are identified to be α(Al), η-Zn, TiB<sub>2</sub> and ε-CuZn<sub>4</sub>. The presence of TiB<sub>2</sub> peaks in all of the three developed composites confirms the formation of TiB<sub>2</sub> within the melt. The relative intensity of the TiB<sub>2</sub> signals increases with the increase of mass fraction of TiB<sub>2</sub>, indicating a feasible control of the mass fraction of the TiB<sub>2</sub> reinforcement by the in situ route. It was implied that, after the addition of the mixed salts into molten aluminum, the following consecutive reactions were possible to take place [17]:



The intermediate product TiAl<sub>3</sub> compound is an unfavorable brittle phase. While TiAl<sub>3</sub> is always present in TiB<sub>2</sub> particulate reinforced composites synthesized by in situ mixed salt routes [18,19], this study did not find any trace of its reflections in the XRD pattern. This is attributed to the presence of Na<sub>3</sub>AlF<sub>6</sub> and KCl which

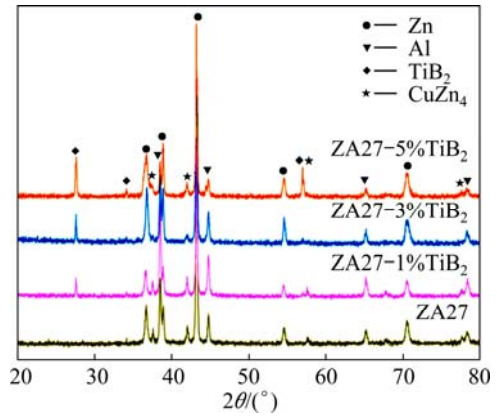


Fig. 2 XRD patterns of ZA27 alloy and developed ZA27–TiB<sub>2</sub> in situ composites

help to finish the above reactions. Also, it is noted that from the XRD analysis, Al<sub>2</sub>O<sub>3</sub>, ZnO and other undesirable compounds, are not detected in the composites. It is thus claimed that the present method is a feasible technique to fabricate ZA27–TiB<sub>2</sub> in situ composites.

The SEM images of the matrix alloy and the developed in situ composites are shown in Fig. 3. The

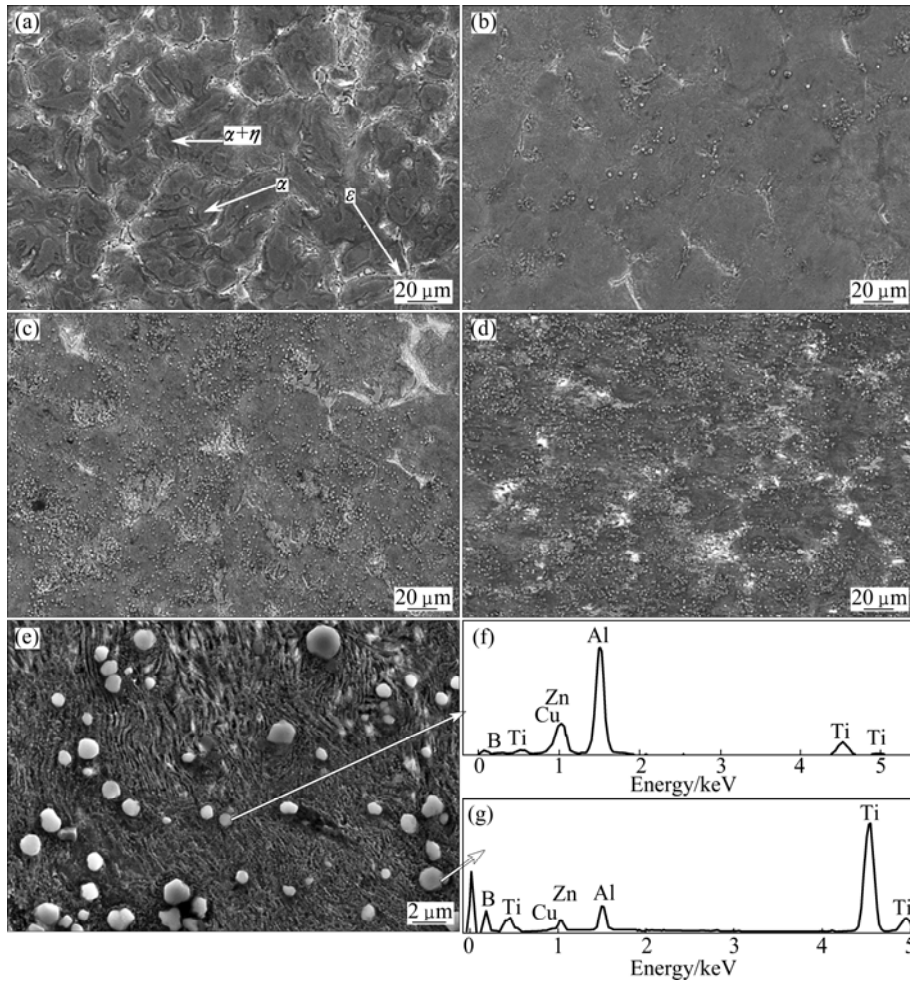


Fig. 3 SEM images of composites: (a) ZA27; (b) ZA27–1%TiB<sub>2</sub>; (c) ZA27–3%TiB<sub>2</sub>; (d) ZA27–5%TiB<sub>2</sub>; (e) ZA27–5%TiB<sub>2</sub> at higher magnification; (f, g) Corresponding EDS results of (e)

microstructure of ZA27 alloy (see Fig. 3(a)) reveals a coarse dendritic structure of primary  $\alpha$  (Al-rich) dendrites, eutectoid  $\alpha+\eta$  ( $\eta$  is Zn-rich) resulted from  $\alpha$ -phase decomposition at 275 °C and intermetallic  $\varepsilon$  (Cu-rich) phase in the interdendritic regions [6]. The  $\text{TiB}_2$  particles distribute uniformly and no agglomeration is observed throughout the matrix. Such kind of particulate distribution is an essential requirement to achieve better mechanical properties of the MMC. It is known that the ceramic particle should suspend in the molten matrix for a long time to obtain homogenous distribution [20]. In our present work, the density difference between ZA27 ( $5.0 \text{ g/cm}^3$ ) and  $\text{TiB}_2$  particle ( $4.5 \text{ g/cm}^3$ ) is small. Therefore, the floating or sinking rate of in situ formed  $\text{TiB}_2$  particles is negligible and  $\text{TiB}_2$  particles could suspend in the molten ZA27 for a long time. Moreover, the good wettability makes  $\text{TiB}_2$  readily embed into the solidification front, thus the  $\text{TiB}_2$  particles are retained inside the grains after solidification. The above said factors lead to more uniform distribution of the reinforcement particles in the final composites.

It is evident from Fig. 3 that grain size of the reinforced composite (Figs. 1(b) and (c)) is smaller than that of the particle-free matrix and decreases with the increase in  $\text{TiB}_2$  content. The grain refinement can be attributed to the following two causes: the  $\alpha$ -phase solidified on  $\text{TiB}_2$  particles which acted as heterogeneous nucleation sites in the initial state of solidification; growing  $\alpha$ -phase was surrounded by hard  $\text{TiB}_2$  particles region, which acted as hard restrictive obstacles against grain growth [20]. Figure 3(e) reveals that the in situ synthesized  $\text{TiB}_2$  particles, evidenced by EDS analysis and the comparison among low magnified images (see Figs. 3(a)–(d)), are hexagonal and spherical in shape, with size distribution ranging from 0.2 to 1.5  $\mu\text{m}$ . This is in agreement with the reports in the available literatures [7,10,20]. These fine particles are much smaller than the ex situ particles in conventional composites, contributing to yielding higher mechanical properties according to the Orowan looping strengthening mechanism. It can also be seen that the interface between  $\text{TiB}_2$  particles and ZA27 matrix is clean. This can be ascribed to two facts: 1) in situ formation of  $\text{TiB}_2$  within the melt reduced the opportunity for oxidation of the particle surface [19]; 2) the heat of reaction and cryolite slag ( $\text{Na}_3\text{AlF}_6$ ) improved the interfacial conditions for bonding and wetting between the particles and the matrix [21].

### 3.2 Mechanical properties of composites

Figure 4 shows the Brinell hardness of the matrix alloy and the experimental composites. It is evident that, as the mass fraction of  $\text{TiB}_2$  particles increases, a significant improvement in the hardness of the developed in situ composites is noticed. An improvement of 3.2%,

7.8% and 16.8% in hardness was observed for 1%, 3% and 5% $\text{TiB}_2$  reinforced ZA27 composites respectively compared with the matrix alloy. The improved hardness was favored by the fine, hard and dispersed  $\text{TiB}_2$  particulates. The strong interface bond, which can efficiently transfer load from the matrix to the particles, may also be responsible for this improvement.

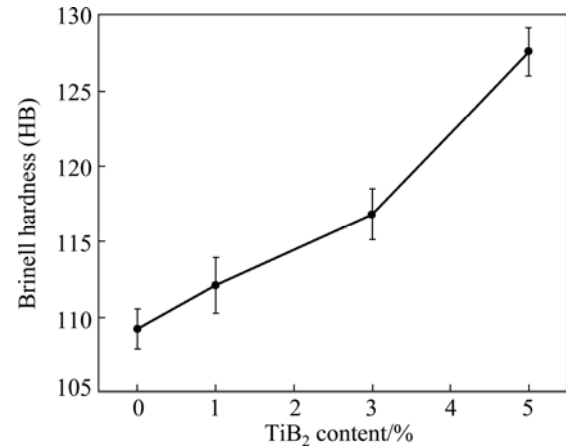


Fig. 4 Influence of  $\text{TiB}_2$  content on hardness of ZA27– $\text{TiB}_2$  in situ composites

The variation of ultimate tensile strength (UTS), yield strength ( $\sigma_{0.2}$ ) and elongation of the developed composites as a function of  $\text{TiB}_2$  content is depicted in Fig. 5. It can be found that UTS and  $\sigma_{0.2}$  increase with the increase of mass fraction of  $\text{TiB}_2$  particles. In contrast, the elongation decreases continuously with the reinforcement content. The UTS of the composite increases from 385 to 434 MPa while the elongation decreases from 4.8% to 3.6% after incorporating 5% in situ  $\text{TiB}_2$  particulates. The experimental results in terms of UTS and ductility are compared with those reported for SiC,  $\text{TiO}_2$ , or  $\text{ZrO}_2$  reinforced ZA27-based MMCs available in literatures [5,6,22]. It is found that, in spite

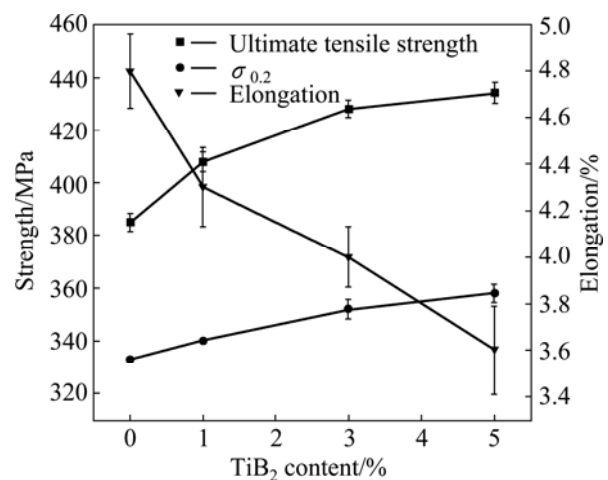


Fig. 5 Effect of  $\text{TiB}_2$  content on tensile strength and elongation of ZA27– $\text{TiB}_2$  in situ composites

of lower content of reinforcement is incorporated, the developed composites exhibit superior tensile properties.

The strengthening of ZA27 by in situ formed  $\text{TiB}_2$  particles can be explained as follows: 1) a large amount of fine  $\text{TiB}_2$  particles well distributed in the matrix act as obstacles to the movement of dislocations during the loading of the composites, it is likely for the dislocation line to loop around the fine  $\text{TiB}_2$  particles by the Orowan looping rather than to cut through them owing to the high elastic modulus (534 GPa) of the particles, thus enhancing the strength of the composites according to the Orowan strengthen mechanism [23,24]; 2) during solidification of the MMCs, appending dislocations are created around  $\text{TiB}_2$  particles due to the difference of the thermal expansion coefficient between the base alloy ( $26 \times 10^{-6} \text{ K}^{-1}$ ) and  $\text{TiB}_2$  particle ( $8 \times 10^{-6} \text{ K}^{-1}$ ), the interaction of different dislocation areas also contributed to the higher UTS [25]; 3) grain boundaries can act as obstacles for dislocation slip as well as dislocation source,  $\text{TiB}_2$  particle refines the grains of matrix, which provides more area to resist the dislocation movement.

The decrease in the elongation of the composites with  $\text{TiB}_2$  content may be related to the prevented plastic deformation of the matrix by the particles and the reduction of ductile matrix content when the mass fraction of  $\text{TiB}_2$  particles is increased. Moreover, the residual stresses generated due to the large difference in thermal expansion coefficient between the matrix and particles would probably contribute to the brittle nature of the composites [5].

The fracture morphologies of the ZA27– $\text{TiB}_2$  composites are presented in Fig. 6. The presence of small dimples and tearing ridge in the unreinforced matrix (see Fig. 6(a)) indicates that the fracture mechanism of the base alloy is principally ductile fracture containing some brittle failure. It can be seen that dimples decrease with the increase of  $\text{TiB}_2$  content while the flat regions exhibit an opposite tendency. Flat regions coupled with tearing ridge indicate that the fracture of composites contains quasi-cleavage fracture, which is consistent with the low elongation of the composites. It is worth noting that, in addition to above said fracture features, shrinkage

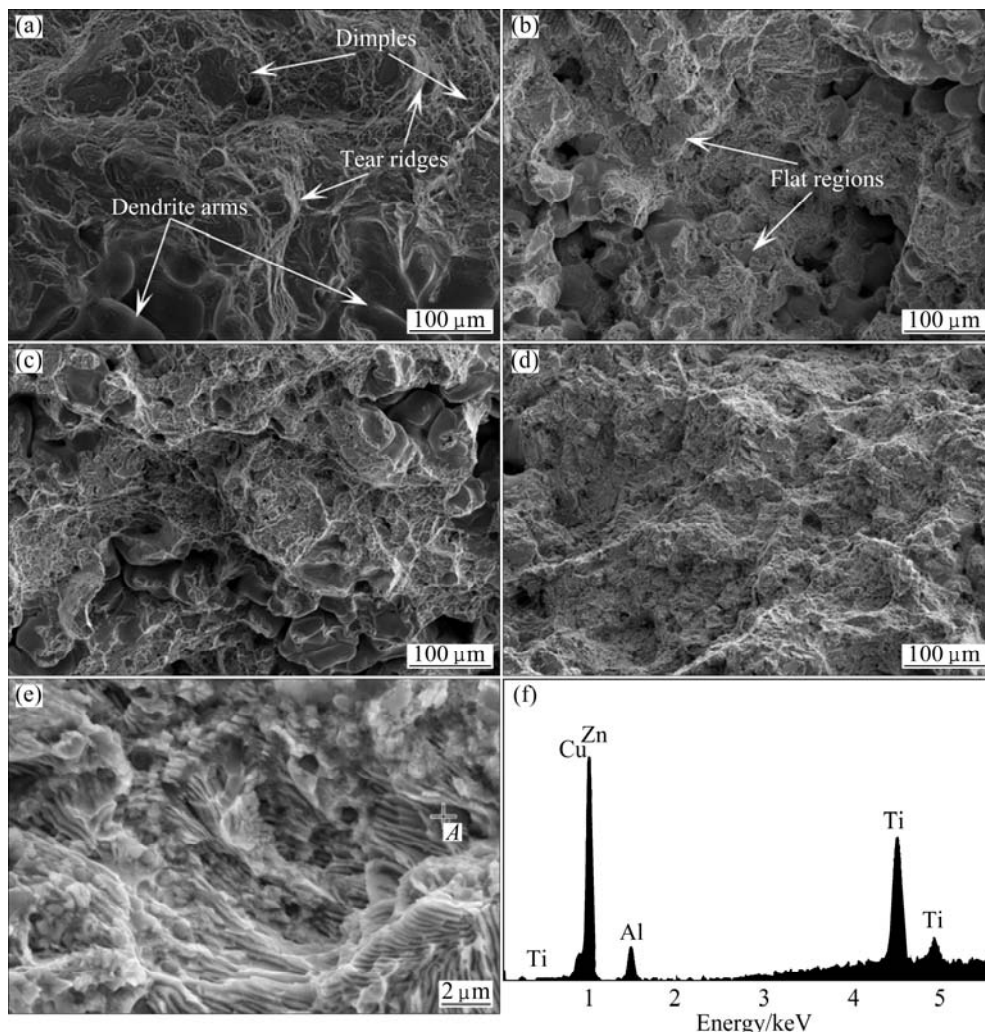


**Fig. 6** SEM images showing fracture surface of composites: (a) ZA27; (b) ZA27–1% $\text{TiB}_2$ ; (c) ZA27–3% $\text{TiB}_2$ ; (d) ZA27–5% $\text{TiB}_2$ ; (e) ZA27–5% $\text{TiB}_2$  at higher magnification; (f) EDS spectrum of spot A in (e)

cavities also present on the fracture surfaces of the matrix, 1% and 3%TiB<sub>2</sub> reinforced composites. This can be attributed to the dendrite segregation in non-equilibrium solidification process. The continuous enrichment of solute in interdendrite residual liquid and subsequent solidification without effective feeding results in weakened grain boundary, which is verified by the exposed dendrite arms inside the cavities. As the TiB<sub>2</sub> content increases, the grain size reduces and the dendrite segregation becomes insignificant, for ZA27–5%TiB<sub>2</sub> (see Fig. 6(d)), which shows a brittle fracture, and no obvious shrinkage cavities are observed. The presence of titanium in EDS spectrum (see Fig. 6(f)) of spot *A* (see Fig. 6(e)) combined with the foregoing XRD analysis confirms that the particles on fracture surface are TiB<sub>2</sub>. Although debonding at some places can be detected, bonding between particles and matrix is generally good, and the majority of particles are well encompassed by the matrix, providing firm evidence of excellent bonding between the matrix and in situ formed TiB<sub>2</sub> particles.

### 3.3 Wear behaviour of composites

The variation of friction coefficient as a function of test duration for the base alloy and in situ composites is plotted in Fig. 7. It is evident that the friction coefficient is decreased by incorporating in situ TiB<sub>2</sub> particles into the matrix. Increasing content of TiB<sub>2</sub> results in a further decrease. This could be attributed to good bonding at the interface and uniform distribution of the particles as evidenced by the SEM images shown in Fig. 3. It has been demonstrated that a uniform particle distribution and a clean matrix/particle interface both lead to a lower friction coefficient [26]. Similar trends have also been reported by other researchers [18,27]. During the sliding process, the matrix surrounding the TiB<sub>2</sub> particles was worn away and all the contacts were provided between the particles and the steel counter face. The gap between

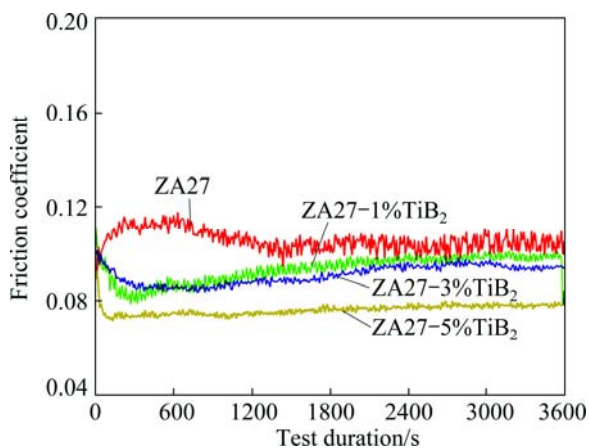


Fig. 7 Variation of friction coefficient with test duration for alloy and composites

the contact surfaces could store oil and help to improve the lubricating condition.

It should be noted that the friction coefficients of the composites initiated with a sharp decrease and then reached a constant level while the base alloy showed a contrary trend during the early stage of wear test, indicating that there was a change in the wear mechanism after introducing the TiB<sub>2</sub> particles into the matrix. It is well known that at the beginning of the test run, contact between the sliding surfaces occurs at only a few highly protruding asperities and the oil film is unstable [3]. As the test proceeds, the area of contact increases and a more stable lubricating layer forms, thereby leading to the decrease of the friction coefficient. In the case of the base alloy, asperity junction took place in the initial stage due to the low hardness and inferior strength. As a consequence, local tearing occurred in the vicinity of the asperities and gave rise to coarse debris which got clogged between the rubbing surfaces (confirmed by the following wear surfaces analysis) and coupled with the rough worn surface, resulting in the initial increase of the curve.

The variation of the wear rate of ZA27–TiB<sub>2</sub> in situ composites as a function of TiB<sub>2</sub> content is depicted in Fig. 8. It is observed that the wear rate decreases dramatically with the increase of TiB<sub>2</sub> content. Incorporating 5% TiB<sub>2</sub> reduces the wear rate of the composite from  $5.9 \times 10^{-3}$  to  $1.3 \times 10^{-3}$  mm<sup>3</sup>/m. This can be attributed to higher hardness of the composites and good interfacial bonding between the matrix and reinforcement, both of which enhance the bearing capacity of the final composite [27]. Furthermore, TiB<sub>2</sub> particles reduce the extent of direct metal-to-metal contact and play the role of bearing load for protecting the matrix during the sliding process.

SEM images of the worn surfaces of ZA27 and the developed in situ composites are shown in Fig. 9.

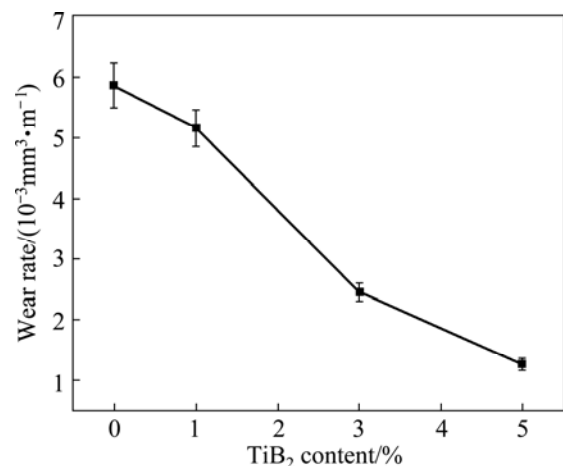
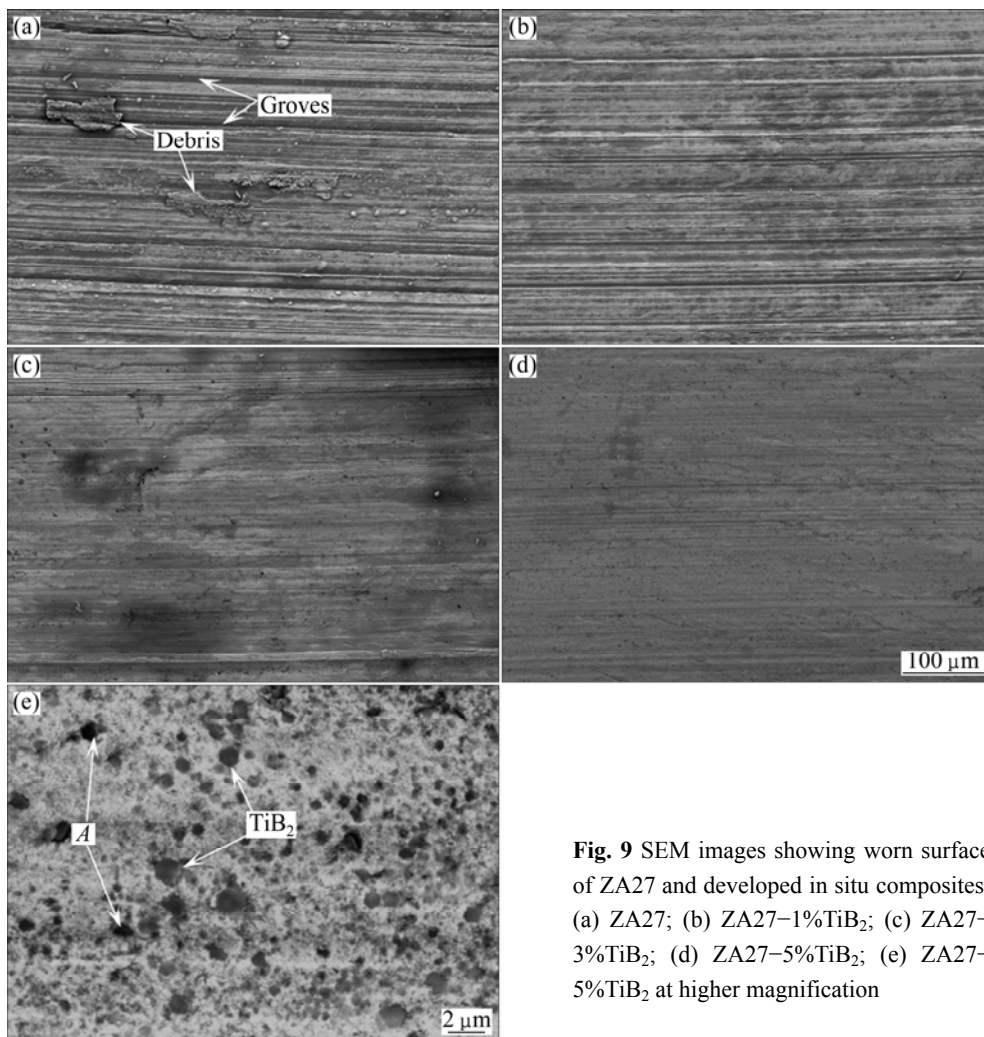


Fig. 8 Influence of TiB<sub>2</sub> content on wear rate of ZA27–TiB<sub>2</sub> in situ composites



**Fig. 9** SEM images showing worn surface of ZA27 and developed in situ composites: (a) ZA27; (b) ZA27–1%TiB<sub>2</sub>; (c) ZA27–3%TiB<sub>2</sub>; (d) ZA27–5%TiB<sub>2</sub>; (e) ZA27–5%TiB<sub>2</sub> at higher magnification

The worn surface of the ZA27 matrix alloy exhibits deep and wide grooves running parallel to one another along the sliding direction. Some coarse debris were worn out and reattached onto the worn surface due to the contact pressure. The composites, to the contrary, revealed narrow grooves and almost flat surfaces. These observations support the lower friction coefficients and wear rates of the composites. Figure 9(e) clearly shows that particles with well-developed hexagonal morphology distributed evenly throughout the surface in spite of a few particles damaged during sliding (region A).

Grooves were formed due to the ploughing of the steel counterpart on the sample surface. The smooth worn surfaces of the in situ composites were attributed to the following factors: 1) verified by the dispersed TiB<sub>2</sub> particles on the worn surface, the strong interfacial bonding between the TiB<sub>2</sub> particles and the matrix minimized the debonding trend of TiB<sub>2</sub> from the matrix alloy, ensuring that these stiff TiB<sub>2</sub> particles effectively resist the ploughing of the counterpart; 2) compared with

the matrix alloy, the developed in situ composites have higher hardness, thus leading to narrow and shallow grooves; 3) the TiB<sub>2</sub> fragments damaged off from individual particles were entrapped in the oil and rolled across the wear surfaces, resulting in three-body abrasive wear [28], in general, three-body abrasion results in a lower wear rate than that of the two-body abrasion [18,28], which was just the case in the wear test of the ZA27 base alloy.

#### 4 Conclusions

1) ZA27–TiB<sub>2</sub> in situ composites were successfully fabricated via in situ mixed salt reaction. The undesirable phases such as brittle compound TiAl<sub>3</sub>, have been completely suppressed. The formation of hexagonal and spherical shaped in situ TiB<sub>2</sub> particles with clean particle–matrix interface and sizes ranging from 0.2 to 1.5 μm was confirmed by XRD and SEM analyses.

2) The composites exhibit a significant improvement in hardness and tensile strength, while a

reduction in elongation, in comparison to the base alloy. The Brinell hardness and UTS of the composites containing 5% TiB<sub>2</sub> are up to HB 128 and 434 MPa, respectively.

3) In situ TiB<sub>2</sub> particles significantly improve wear response of the zinc-based matrix alloy. Both friction coefficient and wear rate decrease dramatically with the increase in TiB<sub>2</sub> content. Friction coefficient and worn surface analyses indicate that there is a change in the wear mechanism in the initial stage of wear test.

## References

- [1] LO S H J, DIONNE S, SAHOO M, HAWTHORNE H M. Mechanical and tribological properties of zinc–aluminium metal-matrix composites [J]. *Journal of Materials Science*, 1992, 27(21): 5681–5691.
- [2] XU Xiao-qing, LI Dr-fu, GUO Sheng-li, WU Xiao-ping. Microstructure evolution of Zn–8Cu–0.3Ti alloy during hot deformation [J]. *Transactions of Nonferrous Metals Society of China*, 2012, 22(7): 1606–1612.
- [3] PRASAD B K. Sliding wear response of a zinc-based alloy and its composite and comparison with a gray cast iron: Influence of external lubrication and microstructural features [J]. *Materials Science and Engineering A*, 2005, 392: 427–439.
- [4] MODI O P, PRASAD B K, JHA A K. Influence of alumina dispersoid and test parameters on erosive wear behaviour of a cast zinc–aluminium alloy [J]. *Wear*, 2006, 260: 895–902.
- [5] ABOU EI-KHAIR M T, LOTF A, DAOUD A, EL-SHEIKH A M. Microstructure, thermal behavior and mechanical properties of squeeze cast SiC, ZrO<sub>2</sub> or C reinforced ZA27 composites [J]. *Materials Science and Engineering A*, 2011, 528: 2353–2362.
- [6] RANGANATH G, SHARMA S C, KRISHNA M, MURULI M S. A Study of mechanical properties and fractography of ZA-27/titanium–dioxide metal matrix composites [J]. *Journal of Materials Engineering and Performance*, 2002, 11(4): 408–413.
- [7] WANG T M, CHEN Z N, ZHENG Y P, ZHAO Y F, KANG H J, GAO L. Development of TiB<sub>2</sub> reinforced aluminum foundry alloy based in situ composites—Part I. An improved halide salt route to fabricate Al–5wt%TiB<sub>2</sub> master composite [J]. *Materials Science and Engineering A*, 2014, 605: 301–309.
- [8] WANG T M, CHEN Z N, ZHENG Y P, ZHAO Y F, KANG H J, GAO L. Development of TiB<sub>2</sub> reinforced aluminum foundry alloy based in situ composites—Part II. Enhancing the practical aluminum foundry alloys using the improved Al–5wt%TiB<sub>2</sub> master composite upon dilution [J]. *Materials Science and Engineering A*, 2014, 605: 22–32.
- [9] YI Hong-zhan, MA Nai-heng, LI Xian-feng, ZHANG Yi-jie, WANG Hao-wei. Heat treating behaviors of in-situ TiB<sub>2</sub>/ZL109 composites [J]. *The Chinese Journal of Nonferrous Metals*, 2005, 15(8): 1184–1188. (in Chinese)
- [10] ZHANG S L, ZHAO Y T, CHEN G, CHENG X N, SHE C J, WANG X Y, WU D N. Effects of in situ TiB<sub>2</sub> particle on microstructures and mechanical properties of AZ91 alloy [J]. *Journal of Alloys and Compounds*, 2010, 494: 94–97.
- [11] LEE J S, KIM N J, JUNG J Y, LEE E S, AHN S. The influence of reinforced particle fracture on strengthening of spray formed Cu–TiB<sub>2</sub> composite [J]. *Scripta Materialia*, 1998, 39(8): 1063–1069.
- [12] LI B H, LIU Y, LI J, GAO S J, CAO H, HE L. Effect of tungsten addition on the microstructure and tensile properties of in situ TiB<sub>2</sub>/Fe composite produced by vacuum induction melting [J]. *Materials and Design*, 2010, 31(2): 877–883.
- [13] GUO M X, SHEN K, WANG M P. Relationship between microstructure, properties and reaction conditions for Cu–TiB<sub>2</sub> alloys prepared by in situ reaction [J]. *Acta Materialia*, 2009, 57(15): 4568–4579.
- [14] XUE J, WANG J, HAN Y F, LI P, SUN B D. Effects of CeO<sub>2</sub> additive on the microstructure and mechanical properties of in situ TiB<sub>2</sub>/Al composite [J]. *Journal of Alloys and Compounds*, 2011, 509(5): 1573–1578.
- [15] CHEN T J, HAO Y, LI Y D, MA Y. Effect of solid solution treatment on semisolid microstructure of dendritic zinc alloy ZA27 [J]. *Materials Science and Technology*, 2008, 24(11): 1313–1320.
- [16] LIU Yang, LI Hong-ying, JIANG Hao-fan, LU Xiao-chao. Effects of heat treatment on microstructure and mechanical properties of ZA27 alloy [J]. *Transactions of Nonferrous Metals Society of China*, 2013, 23(3): 642–649.
- [17] BARTELS C, RAABE D, GOTTSTEIN G, HUBER U. Investigation of the precipitation kinetics in an Al6061/TiB<sub>2</sub> metal matrix composites [J]. *Materials Science and Engineering A*, 1997, 237: 12–23.
- [18] KUMAR S, CHAKRABORTHY M, SUBRAMANYA SARMA V, MURTY B S. Tensile and wear behaviour of in situ Al–7Si/TiB<sub>2</sub> particulate composites [J]. *Wear*, 2008, 265: 134–142.
- [19] LÜ L, LAI M O, SU Y, TEO H L, FENG C F. In situ TiB<sub>2</sub> reinforced Al alloy composites [J]. *Scripta Materialia*, 2001, 45(9): 1017–1023.
- [20] MICHAEL RAJANA H B, RAMABALAN S, DINAHARAN I, VIJAY S J. Synthesis and characterization of in situ formed titanium diboride particulate reinforced AA7075 aluminum alloy cast composites [J]. *Material and Design*, 2013, 44: 438–445.
- [21] LAKSHMI S, LU L, GUPTA M. In situ preparation of TiB<sub>2</sub> reinforced Al based composites [J]. *Journal of Materials Processing Technology*, 1998, 73: 160–166.
- [22] PAN Lei, TAO Jie, LIU Zi-li, CHEN Zhao-feng. Zinc matrix composites prepared by ultrasonic assisted casting method [J]. *Transactions of Nonferrous Metals Society of China*, 2005, 15(S3): 104–109.
- [23] LU L, LAI M O, CHEN F L. Al–4 wt% Cu composite reinforced with in-situ TiB<sub>2</sub> particles [J]. *Acta Materialia*, 1997, 45(10): 4297–4309.
- [24] LEE J S, JUNG J Y, LEE E S, PARK W J, AHN S, KIM N J. Microstructure and properties of titanium boride dispersed Cu alloys fabricated by spray forming [J]. *Materials Science and Engineering A*, 2000, 277: 274–283.
- [25] ZHAO D G, LIU X F, PAN Y C, BIAN X F, LIU X J. Microstructure and mechanical properties of in situ synthesized (TiB<sub>2</sub>+Al<sub>2</sub>O<sub>3</sub>)/Al–Cu composites [J]. *Journal of Materials Processing Technology*, 2007, 189: 237–241.
- [26] THAKUR S K, DHINDAW B K. The influence of interfacial characteristics between SiC<sub>p</sub> and Mg/Al metal matrix on wear, coefficient of friction and microhardness [J]. *Wear*, 2001, 247: 191–201.
- [27] RAMESH C S, AHAMED A. Friction and wear behaviour of cast Al 6063 based in situ metal matrix composites [J]. *Wear*, 2011, 271: 1928–1939.
- [28] GATES J D. Two-body and three-body abrasion: A critical discussion [J]. *Wear*, 1998, 214: 139–146.

## Zn–Al–Cu–TiB<sub>2</sub> 原位复合材料的 显微组织、力学性能及耐磨性

陈 飞, 王同敏, 陈宗宁, 毛 丰, 韩 强, 曹志强

大连理工大学 材料科学与工程学院, 大连 116024

**摘 要:** 采用混合盐法(K<sub>2</sub>TiF<sub>6</sub>, KBF<sub>4</sub>)在反应温度 875 °C 下制备 Zn–Al–Cu–TiB<sub>2</sub> (ZA27–TiB<sub>2</sub>)原位复合材料。研究此复合材料的显微组织、力学性能和耐磨性。微观组织分析表明, 复合材料中的 TiB<sub>2</sub> 颗粒细小, 分布均匀。复合材料的力学性能随着颗粒含量的增加而显著增加, 相对基体合金, 5% TiB<sub>2</sub> 增强复合材料的布氏硬度提高了 HB 18, 抗拉强度提高了 49 MPa。磨损实验结果说明复合材料的摩擦因数和磨损量随着颗粒含量的增加而明显降低, 当 TiB<sub>2</sub> 含量增加到 5%时, 磨损率由  $5.9 \times 10^{-3} \text{ mm}^3/\text{m}$  降低到  $1.3 \times 10^{-3} \text{ mm}^3/\text{m}$ 。摩擦因数和磨损表面形貌变化表明, 由于 TiB<sub>2</sub> 颗粒的引入, 材料在磨损初期的磨损机制发生了变化。

**关键词:** 原位复合材料; TiB<sub>2</sub> 颗粒; 摩擦因数; 磨损率; 力学性能

(Edited by Xiang-qun LI)